Human Molecular Genetics, 2011, Vol. 20, No. 22 **4440–4451**
doi:10.1093/hmg/ddr372
Advance Access published on August 19, 2011

Temporal and cell-specific deletion establishes that neuronal *Npc1* deficiency is sufficient to mediate neurodegeneration

Ting Yu[1], Vikram G. Shakkottai[2], Chan Chung[1] and Andrew P. Lieberman[1,*]

[1]Department of Pathology and [2]Department of Neurology, University of Michigan Medical School, Ann Arbor, MI 48109, USA

Received June 21, 2011; Revised and Accepted August 16, 2011

Niemann-Pick type C (NPC) disease is an autosomal recessive lysosomal storage disorder caused by mutations in the *NPC1* or *NPC2* genes. Loss of function mutations in either gene disrupt intracellular lipid trafficking and lead to a clinically heterogeneous phenotype that invariably includes neurological dysfunction and early death. The mechanism by which impaired lipid transport leads to neurodegeneration is poorly understood. Here we used mice with a conditional null allele to establish the timing and cell type that underlie neurodegeneration due to *Npc1* deficiency. We show that global deletion of *Npc1* in adult mice leads to progressive weight loss, impaired motor function and early death in a time course similar to that resulting from germline deletion. These phenotypes are associated with the occurrence of characteristic neuropathology including patterned Purkinje cell loss, axonal spheroids and reactive gliosis, demonstrating that there is not a significant developmental component to NPC neurodegeneration. Furthermore, we show that these same changes occur when *Npc1* is specifically deleted only in neurons, establishing that neuronal deficiency is sufficient to mediate central nervous system (CNS) disease. In contrast, astrocyte-specific deletion does not impact behavioral phenotypes, CNS histopathology or synaptic function. We conclude that defects arising in neurons, but not in astrocytes, are the determining factor in the development of NPC neuropathology.

INTRODUCTION

Niemann-Pick type C disease (NPC) is a childhood-onset neurodegenerative disorder characterized biochemically by the accumulation of unesterified cholesterol and glycosphingolipids in late endosomes and lysosomes (1). Loss of function mutations in the *NPC1* gene, which encodes a multipass transmembrane protein that is essential for mobilizing cholesterol from the endolysosomal system, disrupt intracellular lipid trafficking in ~95% of NPC patients (2–4). The resulting disease exhibits progressive neuropathology in which intracellular lipid accumulation, abnormally swollen axons, neuron loss and demyelination underlie the occurrence of cognitive impairment, ataxia, seizures and early death (5). Although disease-causing mutations were identified over a decade ago, it remains unknown how disruption of intracellular lipid transport leads to the severe, progressive neurological impairment characteristic of NPC.

Insights into the pathogenesis of central nervous system (CNS) disease have been gleaned from studies of NPC mouse models. Recent pre-clinical therapeutic trials in mice with an insertional mutation that abolishes *Npc1* gene function highlight cyclodextrin as a promising therapeutic candidate. Cyclodextrin circumvents the requirement for Npc1 to clear stored lipids from diseased cells (6), and several studies have shown that a single injection at postnatal day 7 markedly prolongs the lifespan of mutant mice (7–9). In contrast, injections at later ages are less effective (7–9). Although cyclodextrin's therapeutic mechanism remains incompletely understood, this time-sensitive beneficial effect raised the possibility of a critical developmental window for disease.

Much effort has also focused on defining the cell types responsible for CNS degeneration, with the expectation that this is an important first step toward identifying pathogenic mechanisms. Following the demonstration that transgenic expression of Npc1 predominantly in the CNS diminishes

*To whom correspondence should be addressed at: Department of Pathology, University of Michigan Medical School, 3510 MSRB1, 1150 W. Medical Center Drive, Ann Arbor, MI 48109-0605, USA. Tel: +1 7346474624; Fax: +1 73461534441; Email: liebermn@umich.edu

disease severity in *Npc1* null mice (10), several models systems were used to explore the contributions of neurons and glia. Transgenic rescue experiments in NPC mouse and *Drosophila* models (11,12), and co-culture experiments with neurons and glia (13), raised the possibility that astrocytes contribute to neurodegeneration. However, conditional deletion of *Npc1* only in cerebellar Purkinje cells and an analysis of chimeric mice demonstrate that *Npc1* deficiency triggers cell autonomous Purkinje cell loss (14,15). Furthermore, recent studies show that transgenic expression of Npc1 in neurons, but not astrocytes, delays CNS disease, indicating that Npc1 expression by neurons is necessary for nervous system function (16). Whether neuronal or glial deficiency of Npc1 is sufficient to cause NPC neuropathology has not been addressed previously.

To determine the extent to which *Npc1* deficiency during CNS development is necessary for NPC neuropathology and to help define the cell type critical for disease pathogenesis, we used mice containing a conditional null allele of the *Npc1* gene. By employing various Cre lines, we achieved deletion of the *Npc1* gene in a spatial- and temporal-specific manner. Our findings demonstrate that deletion of *Npc1* in the adult is sufficient to cause disease, and show that neurons, but not astrocytes, are the critical cell type for NPC neurodegeneration.

RESULTS

Adult deletion of *Npc1* recapitulates NPC neuropathology

We first sought to determine the extent to which Npc1 deficiency during CNS development is necessary for NPC neuropathology. To answer this question, we utilized mice with a floxed allele of the *Npc1* gene ($Npc1^{flox}$), in which exon 9 is flanked by *loxP* sites. We have shown previously that Cre-mediated deletion of exon 9 yields a null allele that is functionally indistinguishable from the spontaneous null mutant found in the widely used npc^{nih} ($Npc1^{-/-}$) model (14). These mice were bred with transgenic animals expressing a tamoxifen-regulated Cre recombinase under the control of the cytomegalovirus (CMV) promoter ($Cre\text{-}ER^{TM}$) (17). Our breeding strategy generated littermates expressing Cre recombinase that were compound heterozygotes of the conditional *Npc1* allele. To induce Cre-mediated deletion of experimental ($Npc1^{flox/-}$, $Cre\text{-}ER^{TM+}$) and control ($Npc1^{flox/+}$, $Cre\text{-}ER^{TM+}$) mice, both groups were injected with tamoxifen at 6 weeks, an age at which mice are sexually mature and have a fully developed CNS. Following injections, we verified diminished Npc1 expression in the brain by western blot (Fig. 1A). Similar to mice with germline deletion ($Npc1^{\Delta/-}$), mice with adult deletion ($Npc1^{flox/-}$, $Cre\text{-}ER^{TM+}$) expressed no detectable Npc1 protein in all brain regions examined. Additionally, control mice ($Npc1^{flox/+}$, $Cre\text{-}ER^{TM+}$) expressed reduced protein levels after tamoxifen treatment. Our data indicate that this strategy successfully triggered widespread recombination throughout the brain.

The phenotypic consequences of *Npc1* deletion in adults were weight loss, impaired motor function and early death. Following tamoxifen injections at 6 weeks, $Npc1^{flox/-}$, $Cre\text{-}ER^{TM+}$ males and females, but not $Npc1^{flox/+}$, $Cre\text{-}ER^{TM+}$ controls, started to lose weight around 16 weeks (Fig. 1B and C). By 12 weeks, $Npc1^{flox/-}$, $Cre\text{-}ER^{TM+}$ mice exhibited impaired balance beam performance, indicating a motor deficit, which progressed with age (Fig. 1D). The average lifespan of $Npc1^{flox/-}$, $Cre\text{-}ER^{TM+}$ mice was 109 days post-tamoxifen injections, and comparison of the survival curves of $Npc1^{flox/-}$, $Cre\text{-}ER^{TM+}$ mice (adult deletion) with that of $Npc1^{\Delta/-}$ mice (germline deletion) revealed slightly longer survival (Fig. 1E), a finding that may reflect differences in the extent of gene deletion between these groups.

Based on prior analyses of the neuropathology of mice in which *Npc1* deletion occurred in the germline, we next determined whether similar changes occurred following adult deletion. Calbindin staining of sagittal midline cerebellar sections revealed progressive anterior-to-posterior Purkinje cell loss in tamoxifen-treated $Npc1^{flox/-}$, $Cre\text{-}ER^{TM+}$ mice (Fig. 2A). This patterned Purkinje cell loss has been documented previously in $Npc1^{-/-}$ and $Npc1^{\Delta/-}$ mice (14,18). Quantification of Purkinje cell density demonstrated that the rate of neuron loss fits well into a model incorporating a plateau followed by exponential decay (Fig. 2B). The occurrence of an initial plateau was confirmed by comparing $Npc1^{flox/-}$, $Cre\text{-}ER^{TM+}$ mice at 8 weeks with $Npc1^{flox/+}$, $Cre\text{-}ER^{TM+}$ controls at 21 weeks, indicating that there was no Purkinje cell loss 2 weeks after tamoxifen injections (Fig. 2C). Quantification of Purkinje cell density by lobule revealed selective vulnerability of Purkinje cell subpopulations, with cells in anterior lobules degenerating early and those in posterior lobules exhibiting resistance to the toxicity of Npc1 deficiency (Fig. 2D). This survival of Purkinje cells in posterior lobules occurred despite the accumulation of unesterified cholesterol (Fig. 2E). All of these findings are similar to those documented in Purkinje cell-specific *Npc1* null mice ($Npc1^{flox/-}$, $Pcp2\text{-}Cre^{+}$), further supporting the notion that Purkinje cell loss is independent of events during development (14). In addition to cerebellar pathology, widespread axonal spheroids, secondary demyelination, microgliosis and astrocytosis were also present in $Npc1^{flox/-}$, $Cre\text{-}ER^{TM+}$ mice (Fig. 2F). We conclude that deletion of *Npc1* in the adult CNS is sufficient to cause disease and that there is not a significant developmental component to NPC neuropathology.

Astrocyte-specific deletion of *Npc1* does not lead to CNS pathology

We next sought to establish the contribution of distinct CNS cell populations to NPC neuropathology, and began by deleting *Npc1* only in astrocytes. To achieve astrocyte-specific deletion, we used mice expressing a tamoxifen-regulated Cre recombinase under the control of the human glial fibrillary acidic protein (GFAP) promoter ($GFAP\text{-}CreER^{T2+}$) (19). To avoid confounding effects due to GFAP expression by neuronal precursors during development (20), Cre activation was induced by tamoxifen injections at 6 weeks. We confirmed gene deletion by staining brain sections with filipin, a fluorescent dye that marks accumulations of unesterified cholesterol (21). By performing GFAP and filipin co-staining, we confirmed that $Npc1^{flox/-}$, $GFAP\text{-}CreER^{T2+}$ mice, but not $Npc1^{flox/+}$, $GFAP\text{-}CreER^{T2+}$ controls, contained widespread filipin-positive astrocytes throughout the brain (Fig. 3A–C).

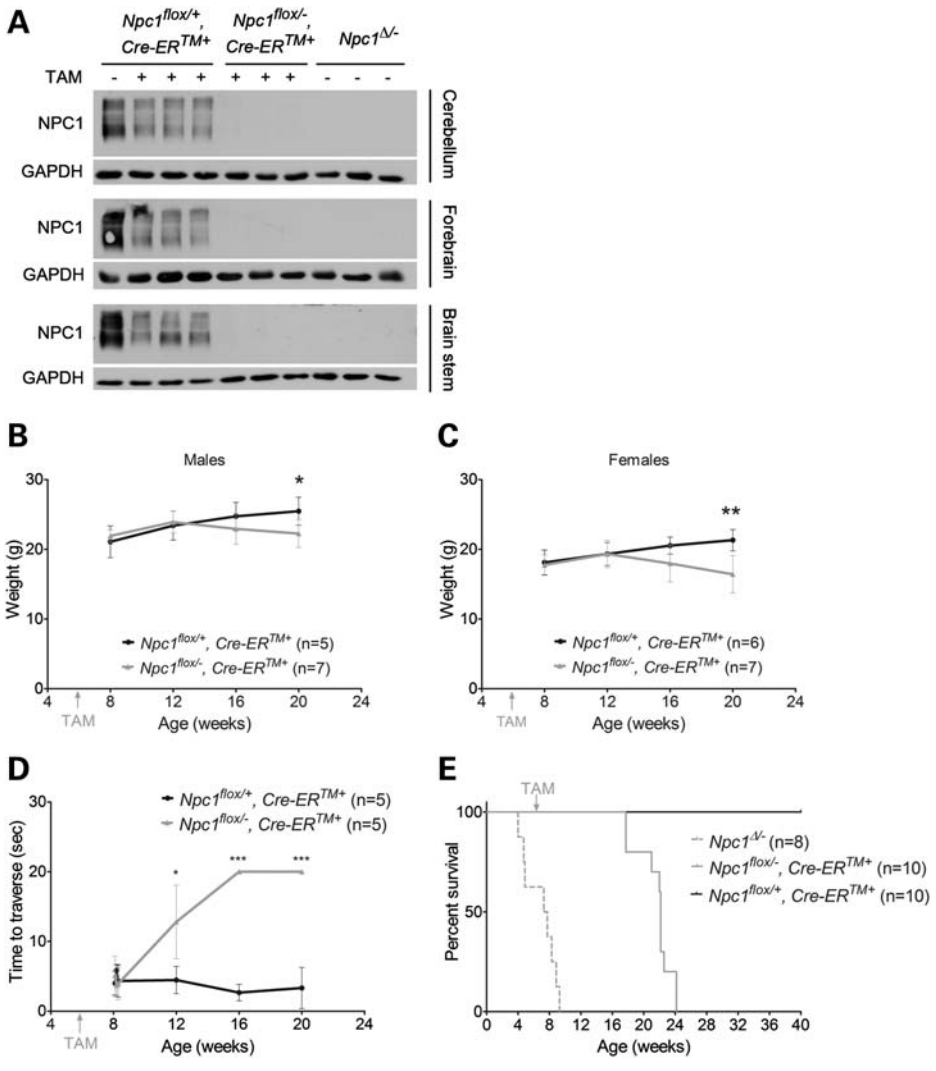

Figure 1. Phenotype of mice following *Npc1* deletion at 6 weeks. (**A**) Western blots of Npc1 protein in mouse brain lysates from three different regions. (**B**–**D**) Weight curves for male (B) and female (C) mice, and age-dependent performance on balance beam (D). Data are mean ± SD. $^{*}P < 0.05$, $^{**}P < 0.01$, $^{***}P < 0.001$. (**E**) Kaplan–Meyer survival curves for mice following *Npc1* deletion at 6 weeks ($Npc1^{flox/-}$, $Cre\text{-}ER^{TM+}$) and for littermate controls ($Npc^{flox/+}$, $Cre\text{-}ER^{TM+}$). For reference, the previously reported survival of mice with germline deletion ($Npc1^{\Delta/-}$) is shown by dashed line (14).

Despite the occurrence of efficient recombination, phenotype analysis did not reveal any differences between astrocyte-specific null mice ($Npc1^{flox/-}$, $GFAP\text{-}CreER^{T2+}$) and their littermate controls ($Npc1^{flox/+}$, $GFAP\text{-}CreER^{T2+}$). Astrocyte-specific null mutants gained weight normally (Fig. 4A and B), showed unimpaired motor performance (Fig. 4C) and exhibited normal survival (Fig. 4D). Similarly, histological examination did not uncover abnormalities in the astrocyte-specific null mutants. Compared with controls, there was no Purkinje cell loss in the cerebellar midline, even at 48 weeks (Fig. 5A and B), nor was there formation of axonal spheroids or evidence of demyelination (Fig. 5C). Additionally, we did not detect activated astrocytes or microglia (Fig. 5C, Supplementary Material, Fig. S1A), despite *Npc1* deletion in astrocytes, supporting the notion that glial reaction occurred secondary to neuron loss. Similarly, while deletion of *Npc1* in primary astrocytes *in vitro* led to the accumulation of free cholesterol, it did not diminish cell survival (Supplementary Material, Fig. S2).

We considered the possibility that *Npc1* deletion in astrocytes impaired neuron function without triggering morphological hallmarks of neuron loss. To test this possibility, we focused on cerebellar glial cells in mice aged <4 weeks. To accomplish this, we generated another cohort of $Npc1^{flox/-}$, $GFAP\text{-}CreER^{T2+}$ mice and $Npc1^{flox/+}$, $GFAP\text{-}CreER^{T2+}$ controls which were injected with tamoxifen at postnatal days 12 and 14. As with mice receiving tamoxifen at 6 weeks, these astrocyte-specific null mice showed no deficits in weight, motor function or survival (Supplementary Material, Fig. S3).

The synapses of cerebellar parallel fibers onto Purkinje cells are strongly wrapped by Bergmann glia, specialized astrocytes in the cerebellum that express a high density of glutamate transporters (22). We determined whether the absence of

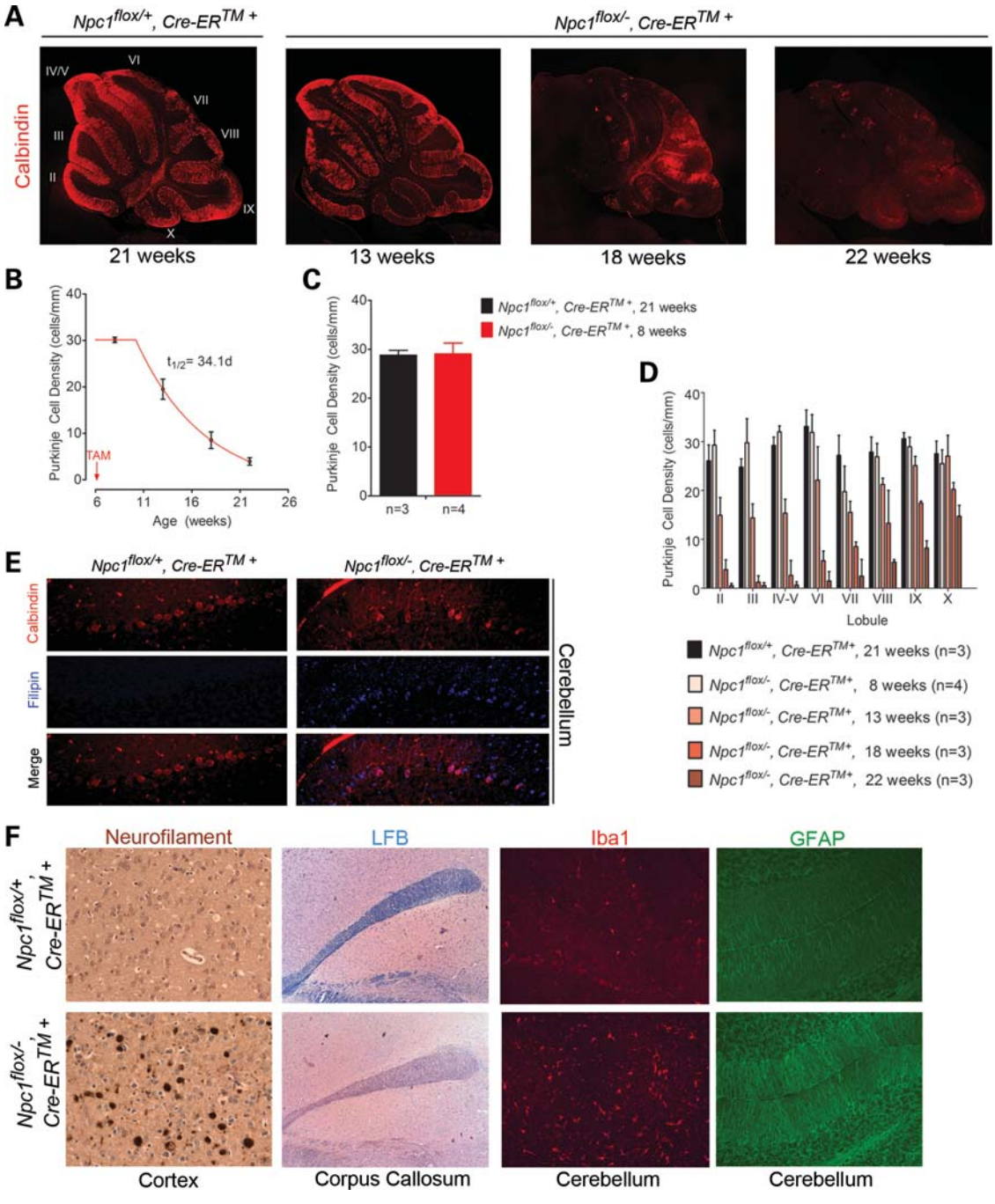

Figure 2. *Npc1* deletion in adult mice recapitulates Niemann-Pick C neuropathology. (**A**) Calbindin immunofluorescence shows progressive anterior-to-posterior Purkinje cell loss in the cerebellar midline of $Npc1^{flox/-}$, $Cre\text{-}ER^{TM+}$ mice following tamoxifen treatment at 6 weeks. Cerebellar lobules are labeled by Roman numerals. (**B**) Quantification of Purkinje cell density in the cerebellar midline over time (mean ± SD). Slope of the decay phase indicates a half-life of 34 days for Purkinje cells. (**C**) Comparison of Purkinje cell density in 8-week-old mutant mice ($Npc1^{flox/-}$, $Cre\text{-}ER^{TM+}$) and 21-week-old littermate controls ($Npc^{flox/+}$, $Cre\text{-}ER^{TM+}$), indicating no Purkinje cell loss 2 weeks after tamoxifen treatment. Data are mean ± SD. $P > 0.05$. (**D**) Quantification of Purkinje cell density in midline cerebellar lobules over time. Data are mean ± SD. (**E**) Calbindin and filipin co-staining reveals accumulation of unesterified cholesterol in cerebellar lobule X of 18-week-old $Npc1^{flox/-}$, $Cre\text{-}ER^{TM+}$ mice (right column), but not in littermate controls (left column). (**F**) Neurofilament (NF) and luxol fast blue (LFB) stains highlight swollen axons in the cortex (NF) and demyelination in the corpus callosum (LFB) of $Npc^{flox/-}$, $Cre\text{-}ER^{TM+}$ mice (bottom row) compared with littermate controls (top row) at 22 weeks. Immunofluorescence demonstrates microgliosis (Iba1) and astrocytosis (GFAP) in the cerebellum of $Npc^{flox/-}$, $Cre\text{-}ER^{TM+}$ mice at 18 weeks (bottom row).

Npc1 triggered glial dysfunction that altered the handling of glutamate at the parallel fiber-Purkinje neuron synapse in cerebellar slices. We assessed glutamatergic synaptic responses using whole-cell patch-clamp recordings from Purkinje neurons in the presence of 50 μM picrotoxin to block inhibitory post-synaptic currents. In response to stimulation of parallel fibers in the molecular layer, we elicited excitatory post-synaptic currents (EPSCs) that increased in amplitude

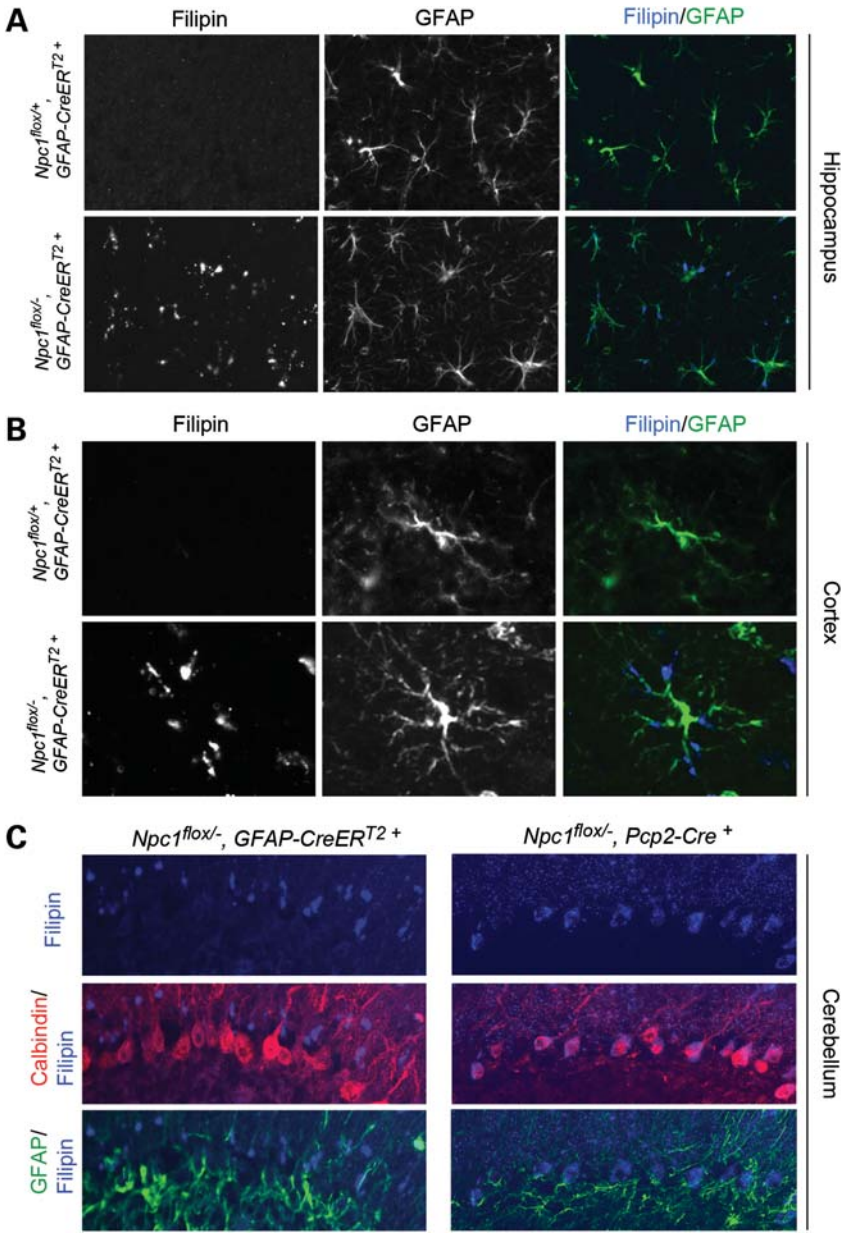

Figure 3. Astrocyte-specific deletion of *Npc1* at 6 weeks leads to the accumulation of unesterified cholesterol in astrocytes. (**A**–**C**) Filipin and GFAP co-staining indentifies the accumulation of unesterified cholesterol in astrocytes of $Npc1^{flox/-}$, $GFAP\text{-}CreER^{T2+}$ mice (bottom rows in A and B) but not in littermate controls (top rows in A and B) after tamoxifen treatment. Shown are representative images of the hippocampus (A), cortex (B) and cerebellum (C). For comparison in (C), co-staining following Purkinje cell-specific deletion ($Npc1^{flox/-}$, $Pcp2\text{-}Cre^{+}$ mice) is shown in the right column.

with increasing stimulus strength. Similar responses (Fig. 5D) and decay time constants (Fig. 5E) were detected in $Npc1^{flox/-}$, $GFAP\text{-}CreER^{T2+}$ and $Npc1^{flox/+}$, $GFAP\text{-}CreER^{T2}$ mice. Since inhibiting glial glutamate transporters slows the decay of parallel fiber EPSCs when many nearby parallel fibers are simultaneously activated (23), we also determined whether the EPSC decay time constant increased with increasing stimulus strength. However, we detected no significant slowing of EPSC decay with increasing stimulation of parallel fibers (Fig. 5F). As Bergmann glia may influence presynaptic transmitter release (24), we determined whether paired-pulse facilitation was altered in the astrocyte-specific null mutants; no difference was detected (Fig. 5G and H). These electrophysiologic studies suggest that the loss of Npc1 in Bergmann glia was not associated with functional alterations in synaptic transmission. Taken together, our analyses indicate that Npc1 deficiency in astrocytes is not a prime contributor to the NPC disease phenotype.

Deletion of *Npc1* in neurons is sufficient to cause neurodegeneration

The fact that mice were not affected by deletion of *Npc1* in astrocytes led us to test whether neurodegeneration in NPC

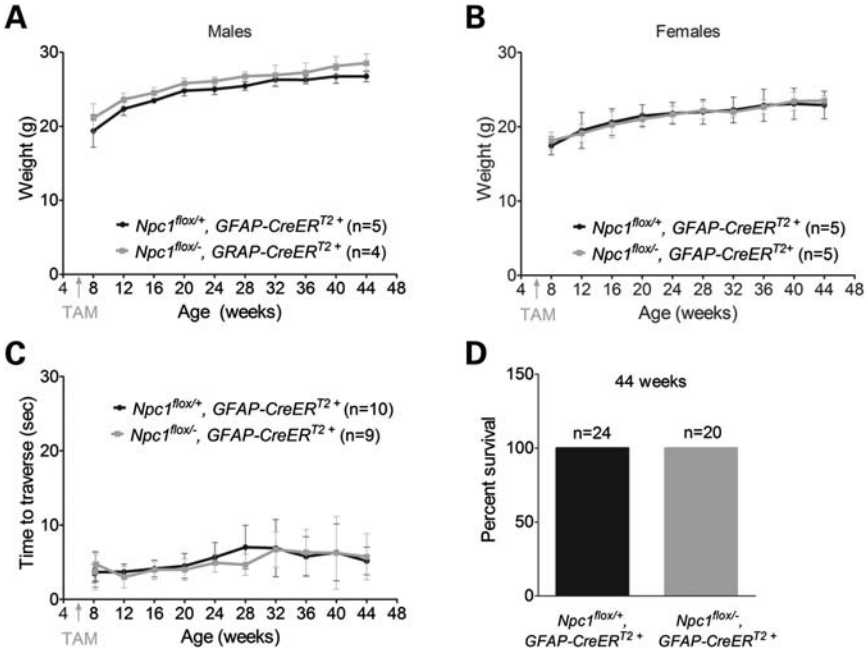

Figure 4. Astrocyte-specific deletion of *Npc1* at 6 weeks does not impair weight, motor function or survival. (**A** and **B**) Weight curves for male (A) and female (B) mice. Data are mean ± SD. (**C**) Age-dependent performance on balance beam. Data are mean ± SD. (**D**) Percent survival at 44 weeks.

is heavily dependent upon toxicity within neurons. To accomplish neuron-specific *Npc1* deletion, we used transgenic mice expressing Cre recombinase under the control of the *Synapsin1* promoter (*Syn1-Cre*) (25). In these mice, Cre is abundantly and specifically expressed in neurons during late embryonic development in a wide range of brain regions, but is minimally expressed in cerebellar Purkinje cells.

Filipin and NeuN co-staining verified that $Npc1^{flox/-}$, $Syn1\text{-}Cre^{+}$ mice, but not $Npc1^{flox/+}$, $Syn1\text{-}Cre^{+}$ controls, developed filipin-positive neurons in multiple brain regions, including the cortex (Fig. 6A) and brainstem (Fig. 6B). Histological examination of liver sections from $Npc1^{flox/-}$, $Syn1\text{-}Cre^{+}$ mice did not reveal an accumulation of foamy macrophages (Fig. 6C), consistent with reports that Cre expression is not leaky in visceral organs. Neuron-specific deletion of *Npc1* reproduced the phenotypic features observed following global gene deletion. $Npc1^{flox/-}$, $Syn1\text{-}Cre^{+}$ mice, but not littermate controls, developed progressive weight loss (Fig. 7A and B), motor deficits in both balance beam (Fig. 7C) and rotarod (Fig. 7D) tests, and early death, with an average lifespan of 105 days (Fig. 7E).

The development of motor impairment occurred in the absence of Purkinje cell degeneration. Histological examination of sagittal midline cerebellar sections revealed no Purkinje cell loss in end-stage $Npc1^{flox/-}$, $Syn1\text{-}Cre^{+}$ mice at 16 weeks (Fig. 8A and B). This finding is consistent with the fact that the *Syn1-Cre* transgene is poorly expressed by Purkinje cells (25). The occurrence of motor deficits in these animals indicates that pathology elsewhere in the nervous system is sufficient to cause this phenotype. In support of this conclusion, $Npc1^{flox/-}$, $Syn1\text{-}Cre^{+}$ mice, but not $Npc1^{flox/+}$, $Syn1\text{-}Cre^{+}$ controls, showed severe axonal pathology with frequent axonal spheroids in the brainstem, loss of myelinated fibers in the corpus callosum and activated microglia and astrocytes in many brain regions (Fig. 8C, Supplementary Material, Fig. S1B). We conclude that deletion of *Npc1* in neurons is sufficient to recapitulate the neuropathological features of NPC mice.

DISCUSSION

Here we used *Npc1* conditional null mutant mice to achieve global deletion of the *Npc1* gene in adults as well as restricted deletion in specific CNS cell types, including astrocytes and neurons. Our findings demonstrate that deletion of *Npc1* in adults is sufficient to recapitulate the disease phenotypes of weight loss, motor deficits and early death. Pathological changes in the CNS of mice following adult deletion were similar to those triggered by germline deficiency and included patterned Purkinje cell loss, axonal pathology and glial activation. Our findings indicate that an impairment of developmental events is not necessary for the occurrence of CNS pathology. Furthermore, our data establish that deletion of *Npc1* in neurons, but not in astrocytes, is sufficient to cause neurodegeneration. The observation that neuronal loss of Npc1 is the primary cause of neuropathology in mice identifies neurons as the critical target cell for future therapeutic interventions.

There has been significant interest in the potential role of astrocytes in the development of NPC neuropathology since the initial observation that these cells robustly express the NPC1 protein (26–28). Astrocytes are an abundant glial cell in the CNS with diverse functions in synaptic transmission (29), neuroinflammation (30) and lipid homeostasis (31). Astrocytic processes are closely associated with synapses,

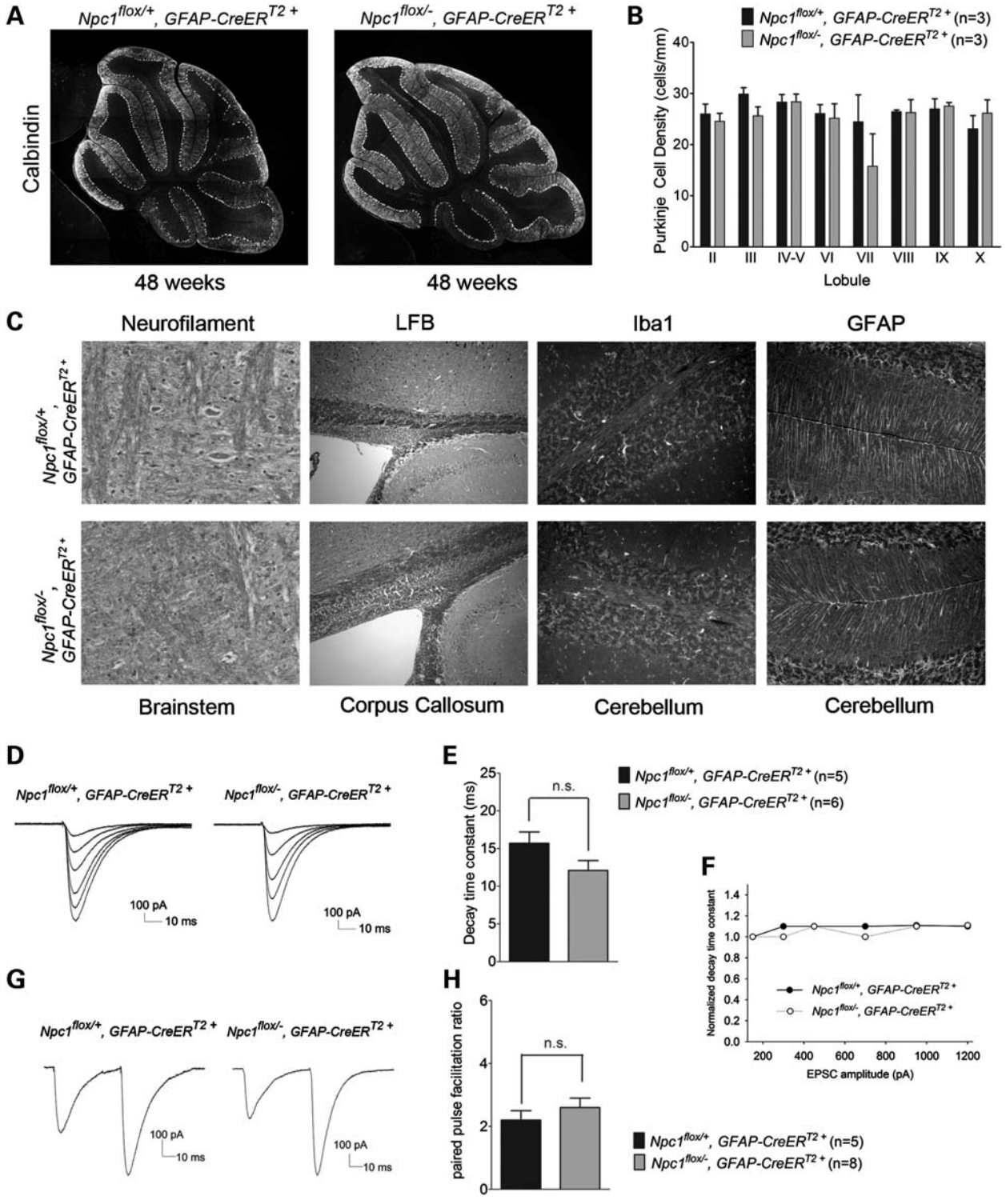

Figure 5. Neuropathology and electrophysiology of Purkinje cells following astrocyte-specific *Npc1* deletion. (**A**) Calbindin staining shows no Purkinje cell loss in 48-week-old Npc1$^{flox/-}$, *GFAP-CreER*$^{T2+}$ mice (right) or littermate controls (left) after tamoxifen treatment at 6 weeks. (**B**) Quantification of Purkinje cell density in midline cerebellar lobules (mean ± SD). (**C**) Neurofilament and luxol fast blue stains reveal no swollen axons (NF) in the brainstem or demyelination (LFB) in the corpus callosum of 48-week-old Npc1$^{flox/-}$, *GFAP-CreER*$^{T2+}$ mice (bottom row) compared with littermate controls (top row). Iba1 and GFAP immunofluorescence identify no gliosis in the cerebellum of these mice. (**D**) Representative traces of parallel fiber-mediated excitatory postsynaptic currents (PF-EPSCs) to increasing stimulus intensity in a Purkinje cell (PC) from *Npc1*$^{flox/+}$, *GFAP-CreER*$^{T2+}$ mice (left) and *Npc1*$^{flox/-}$, *GFAP-CreER*$^{T2+}$ mice (right). (**E**) Quantification of decay time constants of PF-EPSCs with an amplitude of ~300 pA from *Npc1*$^{flox/+}$, *GFAP-CreER*$^{T2+}$ mice ($n = 5$ PCs) and *Npc1*$^{flox/-}$, *GFAP-CreER*$^{T2+}$ mice ($n = 6$ PCs). Data are mean ± SEM, $P > 0.05$. (**F**) Mean decay time constants measured at different EPSC amplitudes, normalized to that of the smallest EPSC for each group. (**G**) Representative traces of PF-EPSCs to pairs of stimuli separated by 50 ms from *Npc1*$^{flox/+}$, *GFAP-CreER*$^{T2+}$ mice (left) and *Npc1*$^{flox/-}$, *GFAP-CreER*$^{T2+}$ mice (right). (**H**) Quantification of the paired-pulse facilitation ratio, expressed as the ratio of the amplitude of the second response to the first one ($n = 5$ PCs from *Npc1*$^{flox/+}$, *GFAP-CreER*$^{T2+}$ mice and $n = 8$ PCs from *Npc1*$^{flox/-}$, *GFAP-CreER*$^{T2+}$ mice). Data are mean ± SEM, $P > 0.05$.

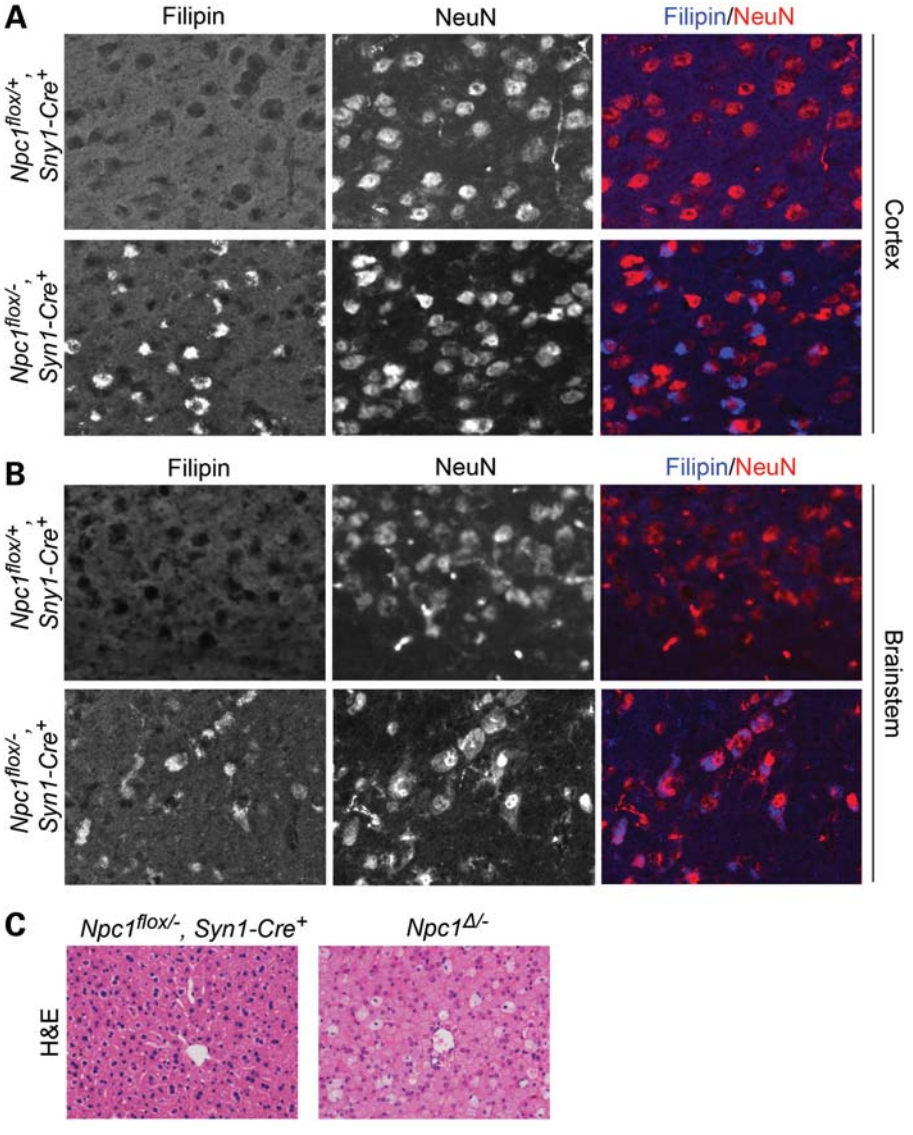

Figure 6. Neuron-specific deletion of *Npc1* leads to accumulation of unesterified cholesterol in neurons. (**A** and **B**) Filipin and NeuN co-staining identifies the accumulation of unesterified cholesterol in neurons of $Npc1^{flox/-}$, $Syn1\text{-}Cre^{+}$ mice (bottom rows) but not in littermate controls (top rows). Shown are representative images of cortex (A) and brainstem (B). (**C**) H&E stain shows foamy macrophages in the liver following germline deletion of *Npc1* ($Npc1^{\Delta/-}$) but not after neuron-specific deletion ($Npc1^{flox/-}$, $Syn1\text{-}Cre^{+}$).

and these cells both promote synaptogenesis by secreting factors, such as lipoproteins (32) and thrombospondins (33), and facilitate synaptic function by contributing to the clearance of extracellular neurotransmitters (34). Astrocytes are also capable of releasing a variety of cytokines, and these inflammatory mediators have been implicated in the development of CNS disease (35). While Npc1 deficiency in astrocytes *in vitro* results in the sequestration of cholesterol in late endosomes and lysosomes, it does not impair the secretion of sterols, including cholesterol (36,37). Nonetheless, given the importance of astrocytes in maintaining brain homeostasis, they have been implicated in NPC neurodegeneration. This notion was supported by prior studies of transgenic mice in which GFAP-promoter driven expression of an *Npc1* transgene extended lifespan of $Npc1^{-/-}$ mice (11). However, a recent analysis of mice expressing a tagged *Npc1* transgene whose expression was clearly restricted to astrocytes showed no phenotypic rescue (16). Here we determined the extent to which deletion of *Npc1* only in astrocytes contributes to CNS disease. Our data show that astrocyte-specific null mutants ($Npc1^{flox/-}$, $GFAP\text{-}CreER^{T2+}$) display no phenotypic abnormalities, histopathological changes or evidence of synaptic dysfunction. These unexpected findings demonstrate that *Npc1* deficiency in astrocytes is not sufficient to mediate disease. Furthermore, the observation that astrocyte-specific null mutants show no glial activation is consistent with prior work, suggesting that gliosis is the consequence, but not the cause of neuronal dysfunction and death.

In marked contrast, neuronal restricted deletion of *Npc1* recapitulates many of the phenotypic and pathological features exhibited by mice with global, germline deficiency. The

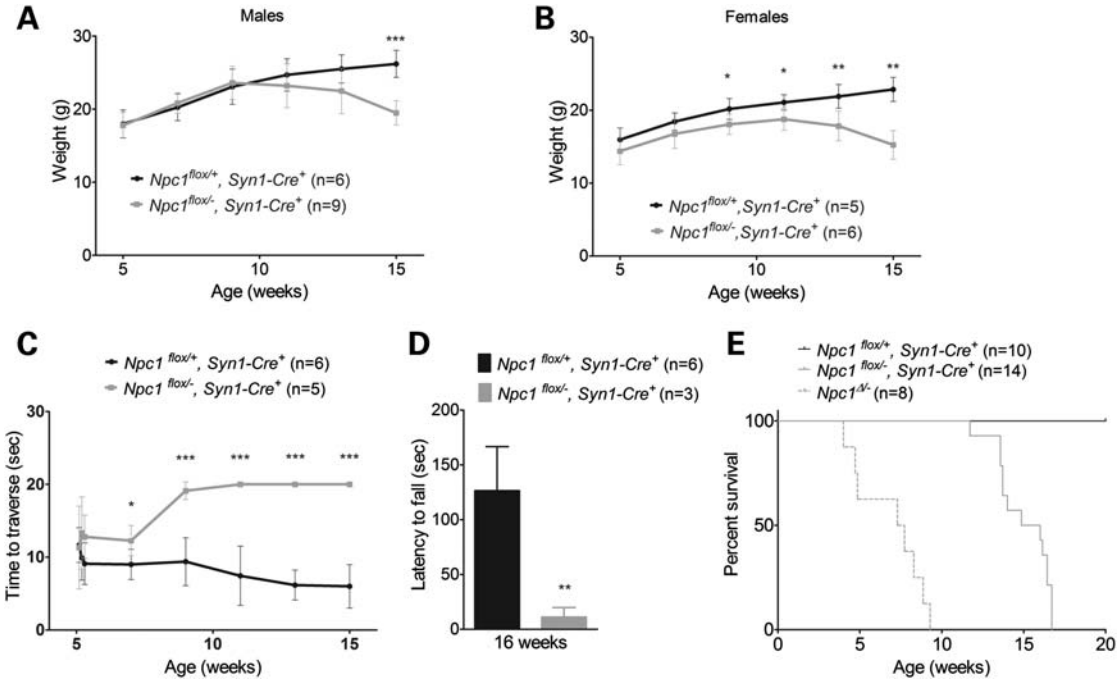

Figure 7. Neuron-specific deletion of *Npc1* impairs weight, motor performance and survival. (**A** and **B**) Weight curves for male (A) and female (B) mice. Data are mean ± SD. $^{*}P < 0.05$, $^{**}P < 0.01$, $^{***}P < 0.001$. (**C** and **D**) Neuron-specific *Npc1* deletion impairs performance on balance beam (C) and rotarod (D). Data are mean ± SD. $^{*}P < 0.05$, $^{**}P < 0.01$, $^{***}P < 0.001$. (**E**) Kaplan–Meyer survival curves for mice following neuron-specific deletion of *Npc1* ($Npc1^{flox/-}$, $Syn1\text{-}Cre^{+}$) or littermate controls ($Npc1^{flox/+}$, $Syn1\text{-}Cre^{+}$). For reference, the previously reported survival of mice with germline deletion ($Npc1^{\Delta/-}$) is shown by dashed line (14).

occurrence of motor impairment in $Npc1^{flox/-}$, $Syn1\text{-}Cre^{+}$ mice was particularly interesting since this occurred in the setting of only limited Cre expression by cerebellar Purkinje cells (25). As such, $Npc1^{flox/-}$, $Syn1\text{-}Cre^{+}$ mice displayed balance beam and rotarod deficits without concurrent Purkinje cell loss. Complementing these findings is our prior analysis of Purkinje cell-specific null mutants that demonstrate motor impairment without other features of the NPC phenotype (14). We conclude that although Purkinje cell loss is sufficient to mediate motor dysfunction, it is not required for it, and pathology elsewhere in the brain likely accounts for this disease manifestation in mice expressing the *Syn1-Cre* transgene. The brainstem, thalamus, cortex and subcortical white matter are abnormal in these mutants, and several of these sites may contribute to the observed phenotype.

The data reported here extend our understanding of disease mechanisms underlying the development of NPC neuropathology. We conclude that neuron dysfunction and loss are the consequence of cell autonomous processes, a notion originally suggested by an analysis of *Npc1*-deficient Purkinje cells (14,15) and supported by neuron-restricted transgenic rescue experiments (16). We find no evidence that astrocytes are primary contributors to disease pathology, despite the existence of multiple potential mechanisms that made them attractive candidates. Finally, our data support the emerging concept that glial reaction and neuroinflammation occur secondary to neuronal injury. Whether the inflammatory mediators they produce contribute to the pathogenic cascade remains to be defined. Taken together, our analysis establishes a critical role for neuronal deficiency of *Npc1* in the development of CNS disease, and compels us to search for therapeutic targets that mediate cell autonomous neurodegeneration.

MATERIALS AND METHODS

Mice

$Npc1^{flox/flox}$ and $Npc1^{\Delta/-}$ mice were generated as previously described (14). Tamoxifen-inducible *CMV-Cre* mice ($Cre\text{-}ER^{TM+}$) (#004682) (17), *Pcp2-Cre* mice (#004146) (38) and *Sny1-Cre* mice (#003966) (25) were from the Jackson Laboratories. Tamoxifen-inducible *GFAP-Cre* mice ($GFAP\text{-}CreER^{T2+}$) (19) were from the Mutant Mouse Regional Resource Center (#016992-MU/H). All mouse strains were backcrossed to C57BL6/J for >10 generations, except *Syn1-Cre* mice which were backcrossed seven generations. Animal use and procedures were approved by the University of Michigan Committee on the Use and Care of Animals.

Tamoxifen induction

Tamoxifen (Sigma) was dissolved in corn oil (Sigma) at 20 mg/ml and stored at −20°C in the dark. The stock solution was warmed to 37°C before injection. Adult mice were injected intraperitoneally with 3 mg (for $Cre\text{-}ER^{TM+}$ mice) or 5 mg (for $GFAP\text{-}CreER^{T2+}$ mice) tamoxifen per 40 g body weight for five consecutive days at 6 weeks. Pups were injected intraperitoneally with 5 mg tamoxifen per 40 g body weight at postnatal days 12 and 14.

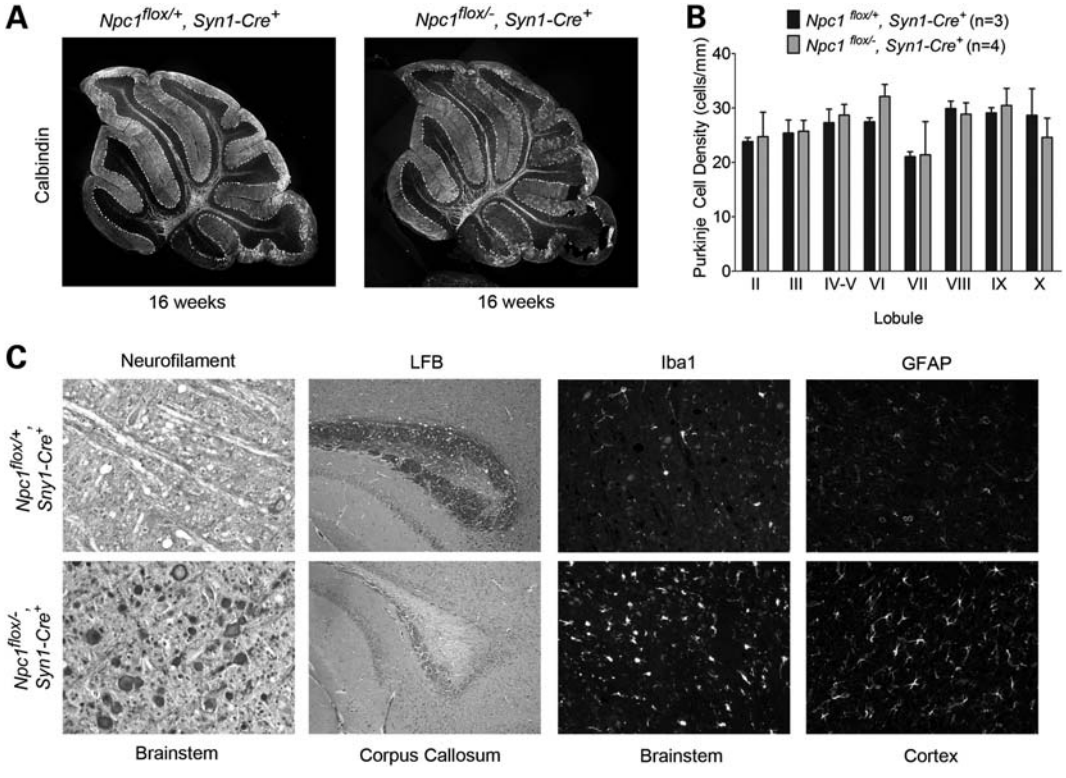

Figure 8. Neuropathology following neuron-specific deletion of *Npc1*. (**A**) Calbindin staining shows no Purkinje cell loss in 16-week-old $Npc1^{flox/-}$, $Syn1\text{-}Cre^{+}$ mice (right) compared with littermate controls (left). (**B**) Quantification of Purkinje cell density in midline cerebellar lobules. Data are mean ± SD. (**C**) Neurofilament (NF) and luxol fast blue (LFB) stains highlight swollen axons in the brainstem (NF) and loss of myelinated axons in the corpus callosum (LFB) of 16-week-old $Npc1^{flox/-}$, $Syn1\text{-}Cre^{+}$ mice (bottom row) but not littermate controls (top row). Immunofluorescence demonstrates microgliosis (Iba1) in the brainstem and astrocytosis (GFAP) in the cortex in $Npc1^{flox/-}$, $Syn1\text{-}Cre^{+}$ mice (bottom row) at 16 weeks.

Phenotype analysis

Motor function was measured using the balance beam and rotarod tests as described previously (14).

Western blot

Brain lysates were homogenized in radio-immunoprecipitation assay buffer (Thermo Scientific) containing complete protease inhibitor cocktail (Roche) and phosphatase inhibitor (Thermo scientific) using a motor homogenizer (TH115, OMNI International). Samples were resolved by 7% or 4 – 20% gradient sodium dodecyl sulfate polyacrylamide gel electrophoresis and transferred to nitrocellulose membranes (BioRad) on a semidry transfer apparatus. Immunoreactivity was detected by Immobilon chemiluminescent substrate (Thermo Scientific). Antibodies used were rabbit anti-NPC1 (1:2000, Abcam), mouse anti-Cre (1:1000, Millipore), rabbit anti-GFAP (1:5000, Dako), rabbit anti-Iba1 (1:2000, Wako) and rabbit anti-GAPDH (1:5000, Santa Cruz).

Histology

Mice were perfused with 0.9% normal saline followed by 4% paraformaldehyde. Brains and livers were removed and post-fixed in 4% paraformaldehyde overnight. Brains were bisected, with the right hemisphere processed for paraffin embedding and the left hemisphere processed for frozen sections. Prior to freezing, brain tissue was cryoprotected in 30% sucrose for 48 h at 4°C. Brains were frozen in isopentane chilled by dry ice and embedded in OCT (Tissue-Tek). Frozen sections were prepared at 14 μm in a cryostat and used for immunofluorescence staining for calbindin (1:1000, Sigma), GFAP (1:1000, Dako) and NeuN (1:500, Millipore). Sections were subsequently stained with filipin by incubating tissue sections for 90 min in phosphate buffered saline with 10% fetal bovine serum plus 25 μg/ml filipin (Sigma). For visualization of staining, secondary antibodies conjugated to Alexa Fluor 594 or Alexa Fluor 488 (Molecular Probes) were used and images were captured on a Zeiss Axioplan 2 imaging system. Paraffin-embedded sections were prepared at 5 μm and used for staining with H&E staining or Luxol fast blue, neurofilament (1:300, Covance) immunohistochemistry and Iba1 (1:1000, Wako) and GFAP (1:1000, Dako) immunofluorescence. Quantification of Purkinje cell loss was performed on H&E stained sections. Counts were normalized to the length of the Purkinje layer, as measured by NIH ImageJ software, and reported as Purkinje cell density.

Primary astrocyte culture

Cerebral hemispheres of 1-day-old mouse pups were dissected for the primary astrocyte culture described previously (39). Tail DNA samples from pups were used for genotyping. After

reaching confluence, cells were trypsinized and plated into 6-well plates for western blot, 12-well plates with cover slips for immunostaining and 96-well plates for XTT assay. Cells were subsequently treated with 5 μM 4-Hydroxytamoxifen (4-OHT, Sigma) after reaching 80% confluence, for four consecutive days to induce Cre-mediated gene deletion. On the following day (designated as 1 day post-deletion), cells were harvested for western blot or immunostaining. XTT assay was performed at different time points as indicated.

XTT assay

XTT assay was carried out using Cell Proliferation Kit II (XTT, Roche) according to the manufacturer's instructions with slight modifications. Briefly, 20 μl of XTT labeling mixture was added to each 96-well containing 100 μl medium. Cells were then incubated at 37°C for 1 h, and the absorbance was measured at 490 nm with the reference at 650 nm.

Electrophysiology

Whole-cell recordings were obtained from Purkinje neurons in 300 μm parasagittal cerebellar slices prepared from 25- to 30-day-old mice. Vibratome sections were cut in ice-cold solution containing (in mM): 87 NaCl, 2.5 KCl, 25 $NaHCO_3$, 1 NaH_2PO_4, 0.5 $CaCl_2$, 7 $MgCl_2$, 75 sucrose and 10 glucose, bubbled with 5% CO_2/95% O_2. Slices were incubated at 33°C in artificial cerebrospinal fluid (ACSF), containing in mM: 125 NaCl, 3.5 KCl, 26 $NaHCO_3$, 1.25 NaH_2PO_4, 2 $CaCl_2$, 1 $MgCl_2$ and 10 glucose, bubbled with 5% CO_2/95% O_2. Purkinje neurons were visualized with infrared differential interference contrast optics on a Nikon upright microscope. Borosilicate glass patch pipettes (with resistances of 2–5 MΩ) were filled with internal recording solution containing (in mM): 130 Cs methanesulfonate, 5 CsCl, 4 NaCl, 2 $MgCl_2$, 5 ethylene glycol tetraacetic acid, 4 Mg ATP, 0.3 Tris-GTP, 10 Na Phosphocreatine, 5 QX-314 and 10 4-(2-hydroxyethyl)-1-piperazineethanesulfonic acid, pH 7.3. Whole-cell recordings were made in ACSF containing 50 μM picrotoxin, 1–5 h after slice preparation using an Axopatch 200B amplifier, Digidata 1400 interface and pClamp-10 software (Molecular Devices, Union City, CA, USA). Series resistance was compensated 50–70%. Cells were rejected if series resistance was >15 mΩ. EPSCs were recorded in voltage-clamp mode at a holding potential of −70 mV. EPSCs were evoked by applying square wave current pulses via a tungsten bipolar electrode to the molecular layer ∼100 μm from the Purkinje neuron of interest. Analog current traces were digitized at 100 kHz. EPSC decay time constants were obtained by fitting the current decay between 10 and 80% of the peak current amplitude to a single exponential as previously described (40).

Statistics

Statistical significance was assessed by unpaired Student's *t*-test (for comparison of two means) or analysis of variance (ANOVA) (for comparison of more than two mean). The Newman–Keuls *post hoc* test was performed to carry out pairwise comparisons of group means if ANOVA rejected the null hypothesis. Statistics were performed using the software package Prism 5 (GraphPad Software). *P*-values <0.05 were considered significant.

SUPPLEMENTARY MATERIAL

Supplementary Material is available at *HMG* online.

ACKNOWLEDGEMENTS

We thank Matthew Elrick and Dr Miriam Meisler for helpful discussions and advice, Dr Kristen Verhey for help with primary astrocyte cultures and Gwen McMichael-Suchanek for help with performing histochemical stains.

Conflict of Interest statement. None declared.

FUNDING

This work was supported by the National Institutes of Health (R01 NS063967 and GM24872-SCS to A.P.L., K08 NS072158 to V.G.S.).

REFERENCES

1. Vanier, M.T. (2010) Niemann-Pick disease type C. *Orphanet. J. Rare Dis.*, **5**, 16.
2. Carstea, E.D., Morris, J.A., Coleman, K.G., Loftus, S.K., Zhang, D., Cummings, C., Gu, J., Rosenfeld, M.A., Pavan, W.J., Krizman, D.B. *et al.* (1997) Niemann-Pick C1 disease gene: homology to mediators of cholesterol homeostasis. *Science*, **277**, 228–231.
3. Kwon, H.J., Abi-Mosleh, L., Wang, M.L., Deisenhofer, J., Goldstein, J.L., Brown, M.S. and Infante, R.E. (2009) Structure of N-terminal domain of NPC1 reveals distinct subdomains for binding and transfer of cholesterol. *Cell*, **137**, 1213–1224.
4. Park, W.D., O'Brien, J.F., Lundquist, P.A., Kraft, D.L., Vockley, C.W., Karnes, P.S., Patterson, M.C. and Snow, K. (2003) Identification of 58 novel mutations in Niemann-Pick disease type C: correlation with biochemical phenotype and importance of PTC1-like domains in NPC1. *Hum. Mutat.*, **22**, 313–325.
5. Higgins, J.J., Patterson, M.C., Dambrosia, J.M., Pikus, A.T., Pentchev, P.G., Sato, S., Brady, R.O. and Barton, N.W. (1992) A clinical staging classification for type C Niemann-Pick disease. *Neurology*, **42**, 2286–2290.
6. Abi-Mosleh, L., Infante, R.E., Radhakrishnan, A., Goldstein, J.L. and Brown, M.S. (2009) Cyclodextrin overcomes deficient lysosome-to-endoplasmic reticulum transport of cholesterol in Niemann-Pick type C cells. *Proc. Natl Acad. Sci. USA*, **106**, 19316–19321.
7. Griffin, L.D., Gong, W., Verot, L. and Mellon, S.H. (2004) Niemann-Pick type C disease involves disrupted neurosteroidogenesis and responds to allopregnanolone. *Nat. Med.*, **10**, 704–711.
8. Liu, B., Turley, S.D., Burns, D.K., Miller, A.M., Repa, J.J. and Dietschy, J.M. (2009) Reversal of defective lysosomal transport in NPC disease ameliorates liver dysfunction and neurodegeneration in the $npc1^{-/-}$ mouse. *Proc. Natl Acad. Sci. USA*, **106**, 2377–2382.
9. Davidson, C.D., Ali, N.F., Micsenyi, M.C., Stephney, G., Renault, S., Dobrenis, K., Ory, D.S., Vanier, M.T. and Walkley, S.U. (2009) Chronic cyclodextrin treatment of murine Niemann-Pick C disease ameliorates neuronal cholesterol and glycosphingolipid storage and disease progression. *PLoS ONE*, **4**, e6951.
10. Loftus, S.K., Erickson, R.P., Walkley, S.U., Bryant, M.A., Incao, A., Heidenreich, R.A. and Pavan, W.J. (2002) Rescue of neurodegeneration in Niemann-Pick C mice by a prion-promoter-driven Npc1 cDNA transgene. *Hum. Mol. Genet.*, **11**, 3107–3114.

11. Zhang, M., Strnatka, D., Donohue, C., Hallows, J.L., Vincent, I. and Erickson, R.P. (2008) Astrocyte-only Npc1 reduces neuronal cholesterol and triples life span of Npc1$^{-/-}$ mice. *J. Neurosci. Res.*, **86**, 2848–2856.
12. Phillips, S.E., Woodruff, E.A. 3rd, Liang, P., Patten, M. and Broadie, K. (2008) Neuronal loss of Drosophila NPC1a causes cholesterol aggregation and age-progressive neurodegeneration. *J. Neurosci.*, **28**, 6569–6582.
13. Chen, G., Li, H.M., Chen, Y.R., Gu, X.S. and Duan, S. (2007) Decreased estradiol release from astrocytes contributes to the neurodegeneration in a mouse model of Niemann-Pick disease type C. *Glia*, **55**, 1509–1518.
14. Elrick, M.J., Pacheco, C.D., Yu, T., Dadgar, N., Shakkottai, V.G., Ware, C., Paulson, H.L. and Lieberman, A.P. (2010) Conditional Niemann-Pick C mice demonstrate cell autonomous Purkinje cell neurodegeneration. *Hum. Mol. Genet.*, **19**, 837–847.
15. Ko, D.C., Milenkovic, L., Beier, S.M., Manuel, H., Buchanan, J. and Scott, M.P. (2005) Cell-autonomous death of cerebellar purkinje neurons with autophagy in Niemann-Pick type C disease. *PLoS Genet.*, **1**, 81–95.
16. Lopez, M.E., Klein, A.D., Dimbil, U.J. and Scott, M.P. (2011) Anatomically defined neuron-based rescue of neurodegenerative Niemann-Pick type C disorder. *J. Neurosci.*, **31**, 4367–4378.
17. Hayashi, S. and McMahon, A.P. (2002) Efficient recombination in diverse tissues by a tamoxifen-inducible form of Cre: a tool for temporally regulated gene activation/inactivation in the mouse. *Dev. Biol.*, **244**, 305–318.
18. Sarna, J.R., Larouche, M., Marzban, H., Sillitoe, R.V., Rancourt, D.E. and Hawkes, R. (2003) Patterned Purkinje cell degeneration in mouse models of Niemann-Pick type C disease. *J. Comp. Neurol.*, **456**, 279–291.
19. Casper, K.B., Jones, K. and McCarthy, K.D. (2007) Characterization of astrocyte-specific conditional knockouts. *Genesis*, **45**, 292–299.
20. Casper, K.B. and McCarthy, K.D. (2006) GFAP-positive progenitor cells produce neurons and oligodendrocytes throughout the CNS. *Mol. Cell Neurosci.*, **31**, 676–684.
21. Bornig, H. and Geyer, G. (1974) Staining of cholesterol with the fluorescent antibiotic "filipin". *Acta Histochem.*, **50**, 110–115.
22. Lehre, K.P. and Danbolt, N.C. (1998) The number of glutamate transporter subtype molecules at glutamatergic synapses: chemical and stereological quantification in young adult rat brain. *J. Neurosci.*, **18**, 8751–8757.
23. Marcaggi, P., Billups, D. and Attwell, D. (2003) The role of glial glutamate transporters in maintaining the independent operation of juvenile mouse cerebellar parallel fibre synapses. *J. Physiol.*, **552**, 89–107.
24. Bordey, A. and Sontheimer, H. (2003) Modulation of glutamatergic transmission by bergmann glial cells in rat cerebellum in situ. *J. Neurophysiol.*, **89**, 979–988.
25. Zhu, Y., Romero, M.I., Ghosh, P., Ye, Z., Charnay, P., Rushing, E.J., Marth, J.D. and Parada, L.F. (2001) Ablation of NF1 function in neurons induces abnormal development of cerebral cortex and reactive gliosis in the brain. *Genes Dev.*, **15**, 859–876.
26. Patel, S.C., Suresh, S., Kumar, U., Hu, C.Y., Cooney, A., Blanchette-Mackie, E.J., Neufeld, E.B., Patel, R.C., Brady, R.O., Patel, Y.C. *et al.* (1999) Localization of Niemann-Pick C1 protein in astrocytes: implications for neuronal degeneration in Niemann- Pick type C disease. *Proc. Natl Acad. Sci. USA*, **96**, 1657–1662.
27. Hu, C.Y., Ong, W.Y. and Patel, S.C. (2000) Regional distribution of NPC1 protein in monkey brain. *J. Neurocytol.*, **29**, 765–773.
28. German, D.C., Liang, C.L., Song, T., Yazdani, U., Xie, C. and Dietschy, J.M. (2002) Neurodegeneration in the Niemann-Pick C mouse: glial involvement. *Neuroscience*, **109**, 437–450.
29. Haydon, P.G. (2001) GLIA: listening and talking to the synapse. *Nat. Rev. Neurosci.*, **2**, 185–193.
30. Farina, C., Aloisi, F. and Meinl, E. (2007) Astrocytes are active players in cerebral innate immunity. *Trends Immunol.*, **28**, 138–145.
31. Vance, J.E., Hayashi, H. and Karten, B. (2005) Cholesterol homeostasis in neurons and glial cells. *Semin. Cell Dev. Biol.*, **16**, 193–212.
32. Mauch, D.H., Nagler, K., Schumacher, S., Goritz, C., Muller, E.C., Otto, A. and Pfrieger, F.W. (2001) CNS synaptogenesis promoted by glia-derived cholesterol. *Science*, **294**, 1354–1357.
33. Christopherson, K.S., Ullian, E.M., Stokes, C.C., Mullowney, C.E., Hell, J.W., Agah, A., Lawler, J., Mosher, D.F., Bornstein, P. and Barres, B.A. (2005) Thrombospondins are astrocyte-secreted proteins that promote CNS synaptogenesis. *Cell*, **120**, 421–433.
34. Danbolt, N.C. (2001) Glutamate uptake. *Prog. Neurobiol.*, **65**, 1–105.
35. Allaman, I., Belanger, M. and Magistretti, P.J. (2011) Astrocyte-neuron metabolic relationships: for better and for worse. *Trends Neurosci.*, **34**, 76–87.
36. Mutka, A.L., Lusa, S., Linder, M.D., Jokitalo, E., Kopra, O., Jauhiainen, M. and Ikonen, E. (2004) Secretion of sterols and the NPC2 protein from primary astrocytes. *J. Biol. Chem.*, **279**, 48654–48662.
37. Karten, B., Hayashi, H., Francis, G.A., Campenot, R.B., Vance, D.E. and Vance, J.E. (2005) Generation and function of astroglial lipoproteins from Niemann-Pick type C1-deficient mice. *Biochem. J.*, **387**, 779–788.
38. Barski, J.J., Dethleffsen, K. and Meyer, M. (2000) Cre recombinase expression in cerebellar Purkinje cells. *Genesis*, **28**, 93–98.
39. Kaech, S. and Banker, G. (2006) Culturing hippocampal neurons. *Nat. Protoc.*, **1**, 2406–2415.
40. Takahashi, M., Kovalchuk, Y. and Attwell, D. (1995) Pre- and postsynaptic determinants of EPSC waveform at cerebellar climbing fiber and parallel fiber to Purkinje cell synapses. *J. Neurosci.*, **15**, 5693–5702.